MSIAC

Munitions Safety Information Analysis Center

Supporting Munitions Safety

O-208

August 2019

FRAGMENTATION FROM DETONATIONS AND LESS VIOLENT MUNITION RESPONSES

Martijn van der Voort, Ernest Baker, Christelle Collet

Presented at

IMEMTS, Sevilla, Spain, 21 - 24 October 2019 &

Parari, Canberra, Australia, 5 - 7 November 2019

Unclassified / Unlimited Distribution

ABSTRACT

An increasing number of munitions now show less violent responses than detonation in cook off or impact scenarios. The detonation of a warhead typically leads to well reproducible fragmentation effects. Deflagrations and explosions may still rupture the munition casing, but fragmentation is typically limited to just a few large fragments with a relatively low velocity. Fragmentation modelling has evolved significantly with increasingly realistic predictions, even for less violent explosions and deflagrations.

Although deflagrating warheads produce only a few fragments, these fragments may reach large distances. Conventional safety distances are not well suited for this situation. Estimates of deflagrating warhead fragment trajectories can be done assuming plate-like fragments. For illustration purposes a simple model of Individual and Group Risk was applied to a case study comparing detonating and deflagrating warheads. A risk based approach holds the advantage that also other relevant aspects can be taken into account, such as a lower probability of initiation, the nature of the ammunition activities, population density, and whether exposed persons are related (personnel) or unrelated (third parties).

Keywords:

Insensitive Munitions, Fragmentation, Individual Risk, Group Risk

---

For contact details, or more information on this and many other topics related to munitions safety visit our website:

www.msiac.nato.int

TABLE OF CONTENTS

INTRODUCTION

An increasing number of munitions now show less violent responses than detonation in cook off or impact scenarios. In order to quantify the safety benefits, MSIAC is working on improvements in the risk management of such munitions.

The Insensitive Munitions European Manufacturers Group (IMEMG) has published an overview of national and international Insensitive Munitions (IM) requirements (Figure 1). This overview shows that for most standardized threats as given in AOP-39 [1] the criterion is to have a response equal to or less than a Burn (type V), Deflagration (IV), or Explosion (III). For these response types only limited quantitative information exists about the physical effects and consequences. This includes primary fragmentation, internal pressure loads and projection of debris from storage structures, as well as external blast (or pressure) waves and thermal effects.

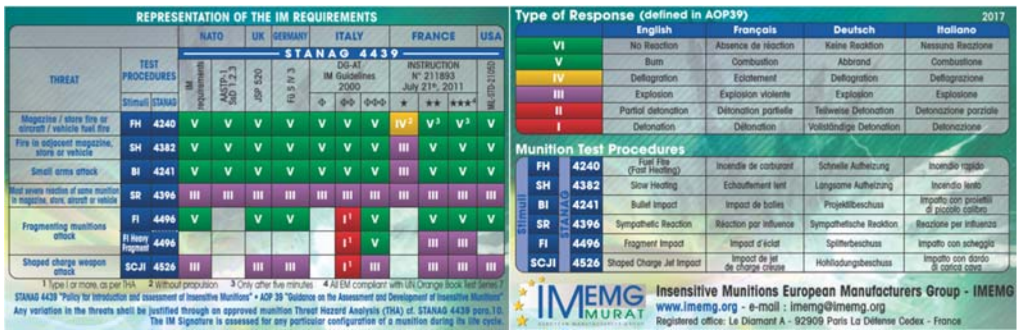

Figure 1: Overview of national and international IM requirements (IMEMG)

An overview of the physical effects from detonations and less violent munition responses was given in various MSIAC reports and papers [2] [3], and more specifically about fragmentation in [4], [5], [6]. The topic was also discussed in detail at the MSIAC Improved Explosives and Munitions Risk Management (IEMRM) workshop, an overview of which will be presented in a companion paper [7] at this symposium.

The current paper will focus on fragmentation effects. The paper starts with a description of fragmentation for the various munition responses and then continues with a discussion of fragmentation models. This is followed by a trajectory analysis of typical fragments generated in a sub-detonative response, and a risk-based approach. The paper closes with conclusions.

1 FRAGMENTATION AND MUNITION RESPONSE

1.1 DETONATION

The detonation of a warhead typically leads to well reproducible fragmentation effects. The launch velocity depends on the explosive reaction rate, warhead burst volume and the fragment explosive contact surface area. While the explosive is reacting, the volume expansion of the explosive products gases pushes the case wall and makes it accelerate. The velocity that it achieves depends on the force history that the case wall receives before the case wall bursts. If the explosive fully detonates, it quickly accelerates the case wall in a reproducible manner. The final fragmentation size is quite small. The number of fragments increases with increasing wall velocity before burst. For a detonating munition, the case wall normally starts to fragment when it has expanded to about two times the original explosive volume [8]. The fragmentation process continues until the case wall has expanded to about three times the original explosive volume. The fragmentation reaches its final velocity sometime during the fragmentation process. This is because the expanding gases are rarefied due to release of pressure when the case wall fractures.

1.2 LESS VIOLENT MUNITION RESPONSES

Deflagrations and explosions may still rupture the munition casing, but fragmentation is typically limited to just a few large fragments with a relatively low velocity. The thickness of these fragments is somewhat thinner than the original case wall due to thinning during the case expansion. The fragment thickness is indicative of the wall casing for the approximate expansion of the case at the time of burst [9]. The largest fragments may also originate from closure parts of the warhead (base plate or nose) and not from the cylindrical part of the casing.

For sub detonative explosive response, the fragments normally do not reach the same velocities as detonating munitions. This is because the explosive reacts more slowly and the case wall breaks before complete reaction of the explosive is complete. As the case wall is moving much slower than a full detonative event, a fewer number of cracks and larger fragments result. These large fragments typically have a plate- or strip-like shape.

The general expectation is that, for less violent munition responses, the effects and consequences will be reduced. Baker et al. [9] have shown that this is not necessarily the case for fragmentation. They describe tests with M107 155 mm Comp B filled artillery shells with a non-standard initiation by a shaped charge. The larger fragments created in the sub-detonative response travelled further due to a lower deceleration by air drag. An example of a 840 g steel fragment reaching 1824 m is given (Figure 2), thereby greatly exceeding the established Hazardous Fragment Distance (HFD) and the Maximum Fragment Distance (MFD)[1] relevant for a detonation of this munition. It was shown that the fragment must have travelled in a spin-stabilised edge-on orientation.

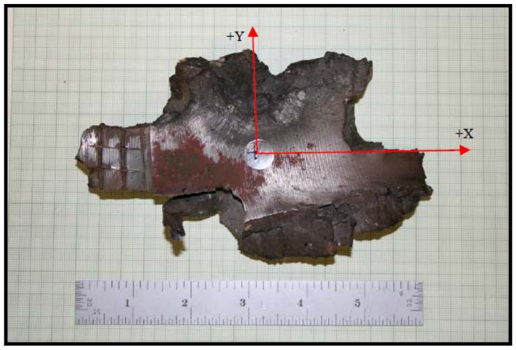

Figure 2: Fragment found at 1824 m after sub-detonative response of an artillery shell (Baker, et al. [9]).

Kinsey [10] provides some experimental characterization of deflagrating munitions during the deflagration process. They quantify the large strip-like fragments that are produced. The fragment velocities are shown to be much slower, having velocities of between 1/3 and 1/10 of the same detonated munition.

Also noteworthy is the development of “dial-a-yield technology” [11]. This technology enables the selection of a desired munitions response between deflagration and detonation. A proof of concept was developed and experiments showed that blast and fragmentation effects could be tuned between low and high output.

[1] HFD = 137 m, MFD = 801 m

2 FRAGMENTATION MODELS

2.1 INTRODUCTION

When dealing with the performance and safety of munitions and warheads, it is important to characterize the mass and velocity distributions of fragments. In the design process of new munitions, the prediction of these parameters plays a significant role to optimize the effects and the overall lethality of the munition. For safety purposes, knowledge about fragmentation is essential in conducting risk management. In this context, analytical models for fragmentation have been developed and used since the late 1940's. The best known are those proposed by Mott, for the mass distribution of fragments, Gurney, for the initial fragment velocity at break-up and Taylor, for the metal projection angle. Some engineering design "toolboxes" which include analytical fragmentation models are: PRODAS, produced by Arrow Tech; SPLIT-X, developed by NUMERICS; and TEMPER, developed by MSIAC. A recent review [4] reveals other analytical models available to predict the above mentioned parameters that could be of interest for specific configurations. More recently, there is an evolution trend from analytical models towards numerical methodologies. Some recent strategies are considered very promising for the fragmentation prediction from munitions, including less than full detonations.

2.2 2D NUMERICAL FRAGMENTATION MODELS

In the 1970's and 1980's, new advanced numerical models enabled more accurate simulations of fragmentation. One of the first "quasi-numerical" models of this kind is probably the one developed by Picatinny Arsenal: CALE/PAFRAG. CALE [12] is the numerical 2D high rate continuum solver and PAFRAG [13] is module including the fragmentation model which uses successive cylindrical "ring-bombs" for the fragmentation distribution calculations.

Developed by LLNL, HEMP [14] is one of the first 2D numerical solvers that included fragmentation modeling. After the calculation duration, which was still quite long for complex geometries, the entire warhead body fragmented instantly when the "average" shell strain reached a pre-determined critical fracture value. This visually results in a "pulverization" of the shell, which is not physically realistic. The lack of representativeness and the long calculation duration for numerical models are probably the reasons why analytical models are still widely used up until now. The results for complex and large 3D geometries also often remain unrealistic due to numerical pulverization of the fragmenting structure. This can occur with uniform parameter distributions, due to a lack of localization causing the entire meshed structure to fail simultaneously.

2.3 3D NUMERICAL FRAGMENTATION MODELS

For three dimensional fragmentation modeling, three dominant methods have been applied; peridynamics, particle hydrodynamics, and stochastically seeded meshed continuum mechanics.

Peridynamics continuum mechanics theory is formulated in terms of integral equations that remain valid in the presence of discontinuities in the displacement field. This feature of the theory is meant to overcome a major obstacle in the modeling of fragmentation using the traditional method which is based on partial differential equations that has difficulties with sharp discontinuities, such as cracks. An added benefit of the peridynamic approach is that crack growth is self-guided: there is no need for supplemental equations that govern crack initiation, velocity, growth direction, branching, and arrest. All of these features emerge directly from the equation of motion and constitutive model. However, it has been noted in results to date that the peridynamics results tend to over predict the number of resulting fragments (Figure 3).

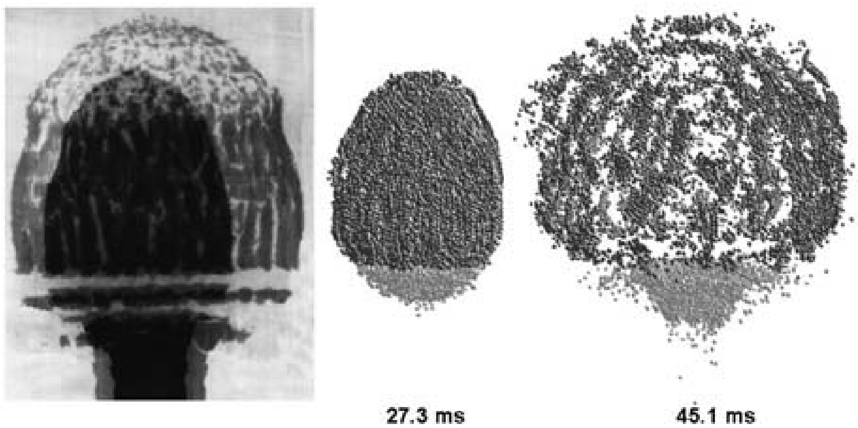

Figure 3: Radiographic image (left) and peridynamics results [15].

Particle hydrodynamics are gridless Lagrangian particle methods originally invented for astrophysical gas dynamics problems. The associated methodology for integrating the continuum partial differential equations has been extended to the dynamic response of solids. The two dominant methods are spherical particle hydrodynamics (SPH) and dual particle hydrodynamics (DPH). DPH attempts to overcome some numerical instabilities observed with SPH. Both methods tend to predict somewhat fewer large mass fragments and more small mass fragments than observed from the experimental data (Figure 4).

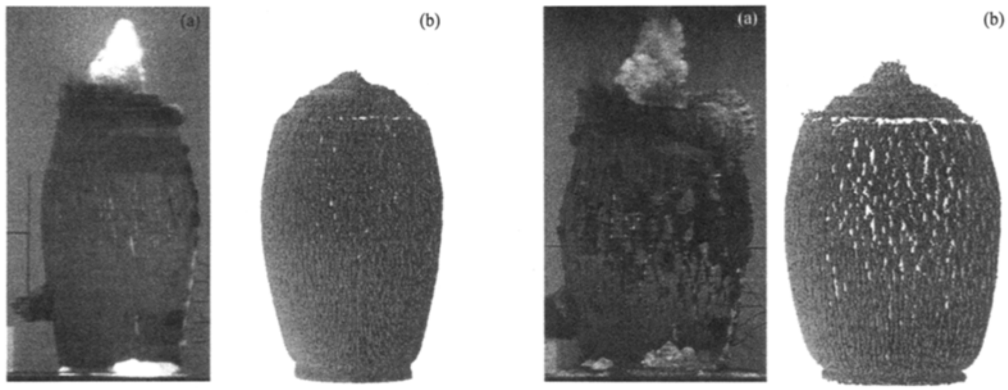

Figure 4: Comparison at 150 μsec (left) and 150 μsec (right) showing onset of fracture and open cracks in both experimental (a) and SPH (b) bomb cases [16].

Stochastically seeded continuum mechanics improves the representation of natural fragmentation in continuum mechanics numerical simulations, by using a stochastic distribution for the mechanical parameters, voids or failure criteria related to the structure. This allows a more physically based localization process to occur, avoiding numerical pulverization. The algorithm developed by Petit in the early 2000's is commonly used for this purpose [17] but some other research teams have optimized it or developed their own algorithms. This stochastic method, coupled with increased computer performances, has made numerical simulations of warhead fragmentation look increasingly realistic [18], [19], [20]. Figure 5 presents an example of a numerical fragmentation pattern that appears quite realistic. This fragmentation modeling method has been shown to predict the larger fragment sizes associated with the lower case velocity and strain rates produced by a deflagration rather than a detonation [21]. Figure 6 presents an example of a fragmentation calculation from a deflagration event.

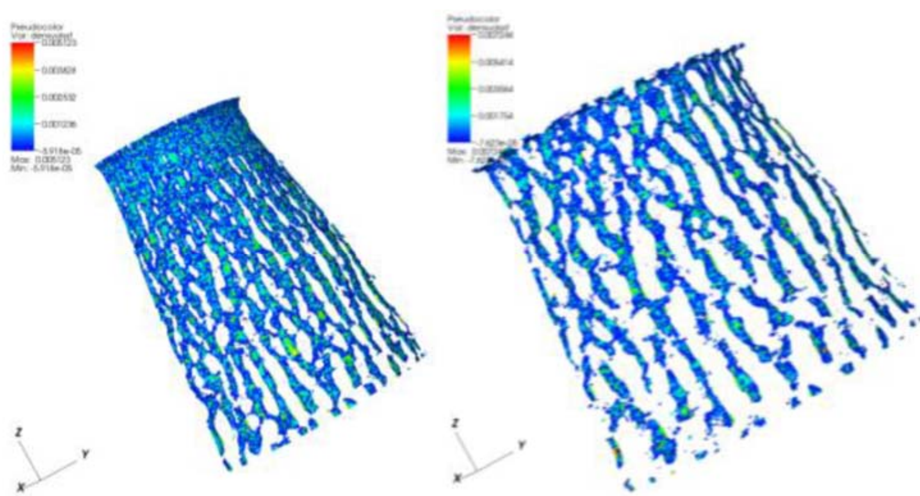

Figure 5: Numerical fragmentation pattern from ALE3D calculation [22].

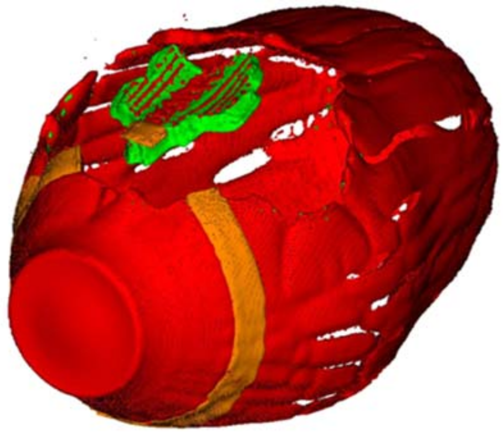

Figure 6: Deflagration fragmentation modeling of a 155mm projectile using ALE3D calculation [9].

3 TRAJECTORY ANALYSIS

In order to get an idea what a sub-detonative response means for various types of warheads, we have conducted a range of trajectory calculations. The large fragments mentioned above have been modeled as rectangular steel plates with a given thickness. In general, the deceleration of an object due to air drag depends on the ratio of the presented area to its mass. A special feature of plate-like fragments is that this ratio is fixed and only depends on the thickness of the plate. This is true for both plates with a face-on orientation and for tumbling plates. A consequence is that the ballistic behavior, and hence the impact distance, is to a good approximation independent of the other two dimensions of the fragment, and as a result independent of its mass. For this analysis we focus on tumbling plates, as this is the most commonly observed mode.

The trajectory code TRAJCAN [23] was used to analyse the trajectories of steel plates with a representative range of warhead casing thicknesses (3 mm, 10 mm, and 30 mm), and a representative range of launch velocities (250 m/s, 500 m/s, 750 m/s, 1000 m/s, 1250 m/s, and 1500 m/s). Launch angles were considered between downward (-90°) to upward direction (+90°). The fragments are assumed to have an initial launch height of 1 m. The results in Figure 7 show a strong dependency on the plate thickness. For thin plates the impact distances are small and relatively insensitive to changes in launch velocity. All predicted distances are below the distance of 1824 m observed in the test by Baker et al. [9], which makes sense because of the assumed spin stabilized edge-on orientation of that fragment. When combined with predictions for the launch velocity, these results can be used to estimate the impact distance for fragments generated by less violent munitions' responses.

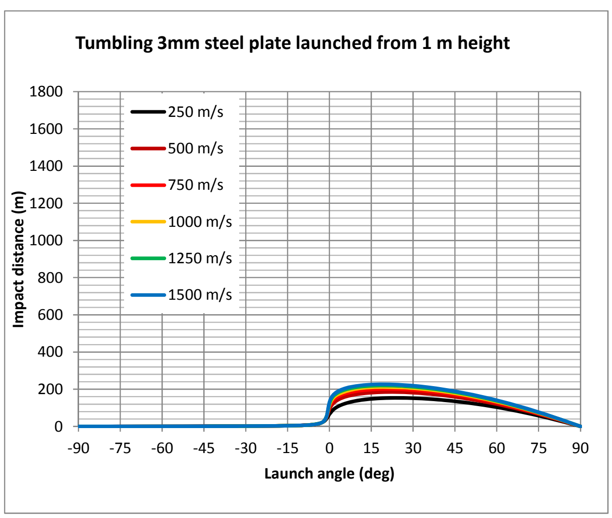

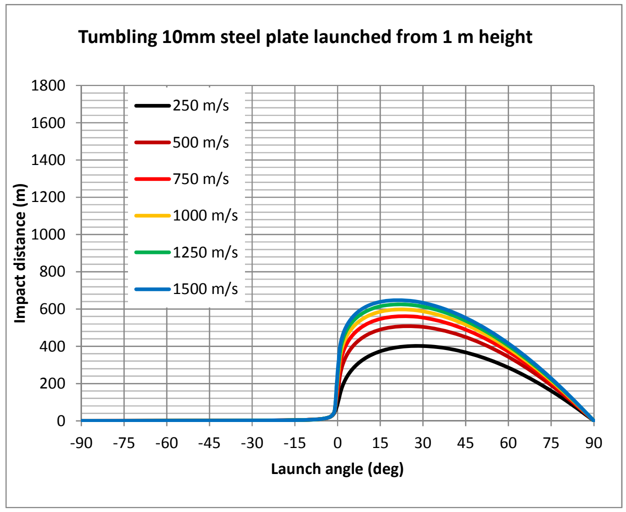

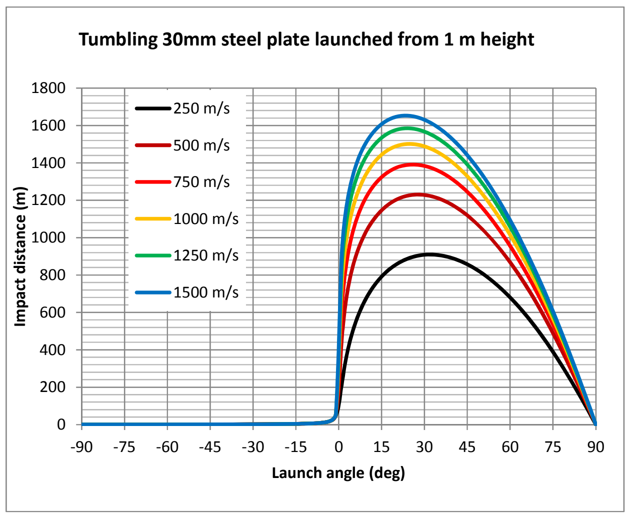

Figure 7: Impact distance versus launch angle for 3, 10 and 30 mm thick tumbling steel plates and a variety of launch velocities [2].

4 RISK-BASED APPROACH TO DEFLAGRATING WARHEADS

4.1 COMMONLY USED FRAGMENTATION RELATED SAFETY DISTANCES

Commonly used "safety" distances for fragmenting munitions are given in the US TP16 [24], and NATO AASTP-1 [25]:

- Maximum Fragment Distance (MFD) for intentional detonations
- Hazardous Fragment Distance (HFD) for accidental detonations. The HFD is the distance at which the number of hazardous fragments has decreased to 1 per 56 m^2, or about a 1 % hit probability for an average person.

These distances are relevant for situations where primary fragmentation is the main hazard, such as in the open or in light storage. Deflagrating warheads that produce a few fragments but which reach large distances raise the question whether the concepts of MFD and HFD are still suitable. On the one hand, the MFD may be very large, on the other hand, due to the small number of (large) fragments, the hit probability and consequently the HFD may be relatively small. This observation raises the question what is an appropriate methodology to determine safety distances. As a result, we have explored the potential of two alternative metrics; the Individual Risk (IR) and Group Risk (GR), and applied it to a case study with two types of warheads [5], [6].

4.2 PROBABILITY OF FATALITY

An essential parameter of the calculation of IR and GR is the probability of fatality given the event takes place. As an illustration we will use a very simple model that assumes the hemispherical expansion of a fragment cloud. All fragments are equal and assumed to be lethal when impacting a person. Fragment trajectories are straight lines, no curvature or protection measures are taken into account. Based on these assumptions we can write the probability of fatality (P_f) as:

$$P_f(r) = \begin{matrix} 1 \; if \; r \le R_L \\ \frac{N \cdot S}{2 \cdot \pi \cdot r^2} \; if \; R_L < r \le MFD \end{matrix} \qquad \text{Eq.1}$$

With N the total number of fragments, S the human body area (typically 0.56 m^2), and r the distance. R_L is the distance with a probability of fatality of 100%, and can be written as:

$$R_L = \sqrt{\frac{N \cdot S}{2 \cdot \pi}} \qquad \text{Eq. 2}$$

From Eq. 1 we can also derive the HFD by setting P_f equal to 0.01 (probability of fatality 1%).

$$HFD = \sqrt{\frac{N \cdot S}{2 \cdot \pi \cdot 0.01}} \qquad \text{Eq. 3}$$

We will now consider the two cases as outlined in Table 1. The first case is a conventional warhead which shows a detonation response to IM threats. It produces numerous (5,000) fragments and has a MFD of "only" 1 km. The second case deals with a warhead with a deflagration as the most severe response. The deflagrating warhead has few (20) fragments but a very large MFD of 2 km. Table 1 gives the calculated 1% and 100% lethal distances, and Figure 8 gives P_f as a function of distance.

Table 1: Case study input and output.

Parameter	Symbol	Case 1 Detonating warhead	Case 2 Deflagrating warhead
Number of fragments (-)	N	5,000	20
Maximum Fragment Distance (m)	MFD	1,000	2,000
100% lethal distance (m)	RL	21	1.3
1% lethal distance (m)	HFD	211	13

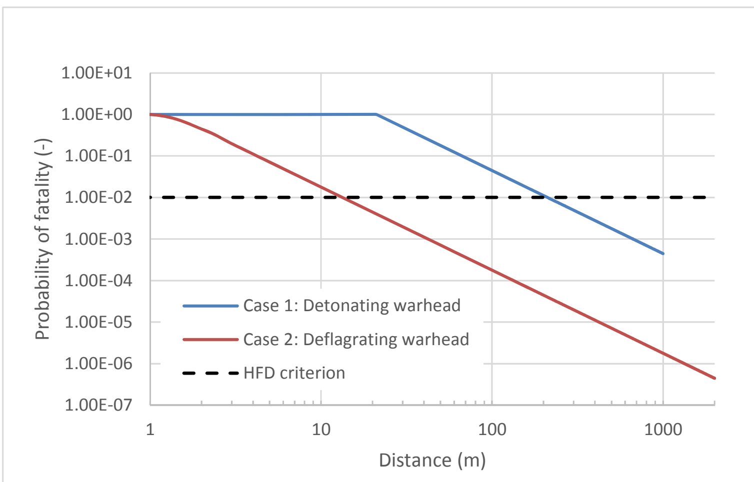

Figure 8: Probability of fatality versus distance for two cases

4.3 ANNUAL PROBABILITY OF EVENT

The second important parameter for the calculation of IR and GR is the annual probability (frequency) of event. **Table 2** presents values from the US for various ammunition activities (e.g. disposal, assembly, testing, manufacture, inspection, (un)loading, and storage) [26]. These values are based on an analysis of historical data (number of accidents divided by combined time duration). Initially the values were presented dependent on Compatibility Group, but this was later changed to Hazard Division. Expert opinion has been used to estimate a probability reduction of e.g. a factor of 100 between HD1.1 and HD1.6.

Table 2: Frequency of event assumed by the US [26].

P(e) Tables: DDESB TP-14 Rev 4
(affected by Compatibility Group)

PES used primarily for:	Probability of Event (PES-year) I	II	III
Burning Ground / Demilitarization / Demolition / Disposal	2.4E-02	2.4E-03	8.1E-04
Assembly / Disassembly / LAP / Maintenance / Renovation	4.7E-03	4.7E-04	1.6E-04
Lab / Test / Training	4.3E-03	4.3E-04	1.4E-04
Manufacturing	1.7E-03	1.7E-03	1.7E-03
Inspection / Painting / Packing	8.2E-04	8.2E-05	2.7E-05
Loading / Unloading	5.7E-04	5.7E-05	1.9E-05
In-Transit Storage (hrs – few days)	3.0E-04	1.0E-04	3.3E-05
Temporary Storage (1 day - 1 mth)	1.0E-04	3.3E-05	1.1E-05
Deep Storage (1 month - year)	2.5E-05	2.5E-05	2.5E-06

Elements	Compatibility Group
I	L, A, B, G, H, J, F
II	C
III	D, E, N

Notes: The elements in the matrix comprise Compatibility Groups. Definitions of the Compatibility Groups can be found in DoD 6055.09-M.

P(e) Tables: DDESB TP-14 Rev 5
(function of Hazard Division)

Activity	HD 1.1/ 1.2/1.5	HD 1.3	HD1.6
Assembly / Disassembly / LAP / Maintenance / Renovation	5.37E-04	1.61E-03	5.37E-06
Burning Ground / Demil / Demolition / Disposal		7.78E-03	
Lab / Test		9.75E-04	
Training	9.75E-04	2.92E-03	9.75E-06
Loading / Unloading	3.15E-05	9.45E-05	3.15E-07
Inspection / Painting / Packing	2.05E-04	6.16E-04	2.05E-06
Manufacturing		1.90E-03	
Storage	1.20E-05	3.59E-05	1.20E-07

For the first case we will assume a characteristic value for case 1 of 1E-5/year. For the second case we may expect a lower probability. Because of the uncertainties we will split this case up in 2a (equal probability as detonating warhead) and 2b (100 times lower probability).

4.4 INDIVIDUAL RISK

The Individual Risk (IR) is the multiplication of the annual probability of event with the probability of fatality.

$$IR(r) = P_e \cdot P_f(r) \qquad \text{(1/year)} \qquad \text{Eq. 4}$$

US acceptance criteria for the IR are 1E-4/year (related persons) and 1E-6/year (unrelated persons) [27]. The IR for case 1, 2a and 2b has been compared with these criteria in Figure 9. The distances beyond which the criteria are met are given in Table 3. For unrelated persons exposed to risk from a detonating warhead, there is a substantial distance of 66 m to meet the criteria. For the deflagrating warhead, it is a few meters (case 2a) or the criterion is always met (case 2b).

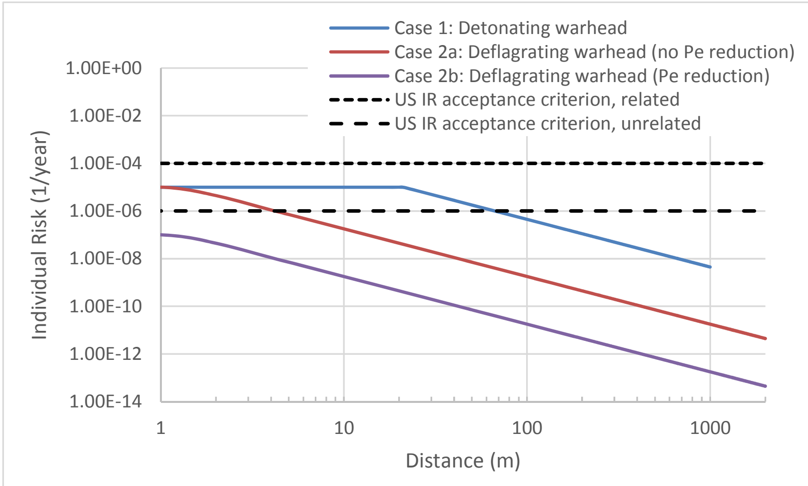

Figure 9: Individual Risk for case 1 and 2 (a and b)

Table 3: Case study input and output (continued)

Parameter	Symbol	Case 1 Detonating warhead	Case 2a Deflagrating warhead No Pe reduction	Case 2b Deflagrating warhead Pe reduction
Probability of event (1/year)	Pe	1E-5	1E-5	1E-7
Distance to IR criterion for related persons (m)	R_{IR10-4}	Criterion always met	Criterion always met	Criterion always met
Distance to IR criterion for Unrelated persons (m)	R_{IR10-6}	66	4.2	Criterion always met

4.5 GROUP RISK

The Group Risk (GR) considers the number of fatalities in a group of persons. For simplicity we will assume that between the warhead and the MFD persons are present with a uniform population density σ (1/m^2). This is illustrated in Figure 10.

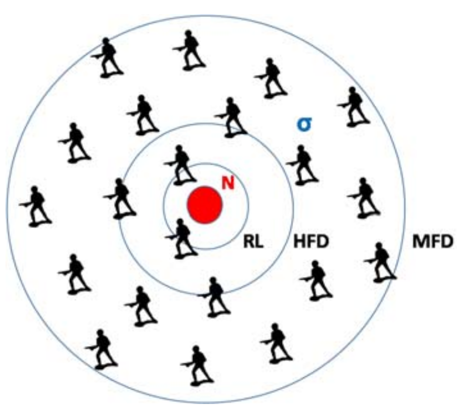

Figure 10: Illustration of Group Risk calculation for related persons.

The expected number of fatalities can be calculated as follows:

$$N_f = \int_0^{MFD} P_f(r) \cdot 2 \cdot \pi \cdot r \cdot \sigma \cdot dr = \int_0^{R_L} 2 \cdot \pi \cdot r \cdot \sigma \cdot dr + \int_{R_L}^{MFD} \frac{N \cdot S}{2 \cdot \pi \cdot r^2} \cdot 2 \cdot \pi \cdot r \cdot \sigma \cdot dr$$

This leads to:

$$N_f = N \cdot S \cdot \sigma \cdot \left[\frac{1}{2} + ln\left(MFD \cdot \sqrt{\frac{2 \cdot \pi}{N \cdot S}}\right)\right] \qquad \text{Eq. 5}$$

The expected number of fatalities is plotted against population density in Figure 11 for case 1 and 2.

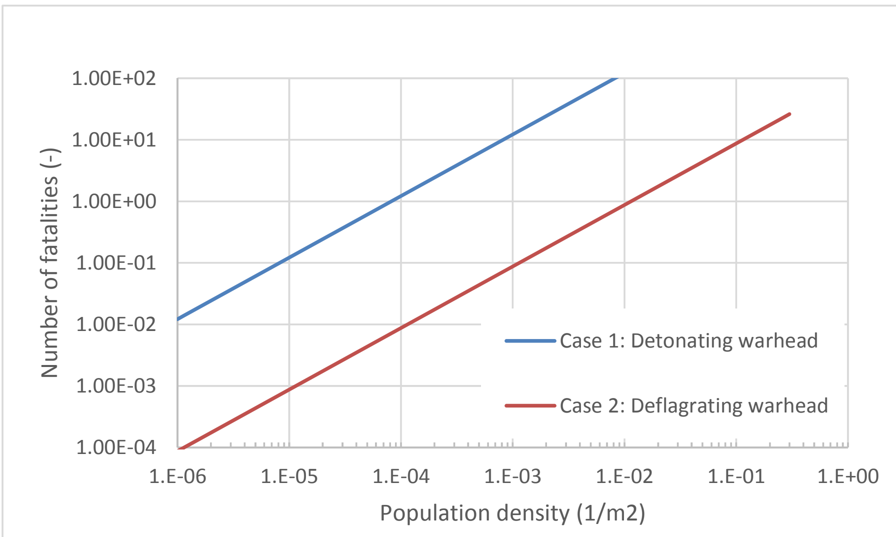

Figure 11: Expected number of fatalities versus population density for case 1 and 2

The Group Risk follows from multiplication of the number of fatalities with the probability of event.

$GR = P_e \cdot N_f$ (1/year) Eq. 6

In Figure 12 we compare case 1, 2a and 2b with the US criterion for GR to related persons (1E-3/year) and unrelated persons (1E-5/year) [27].

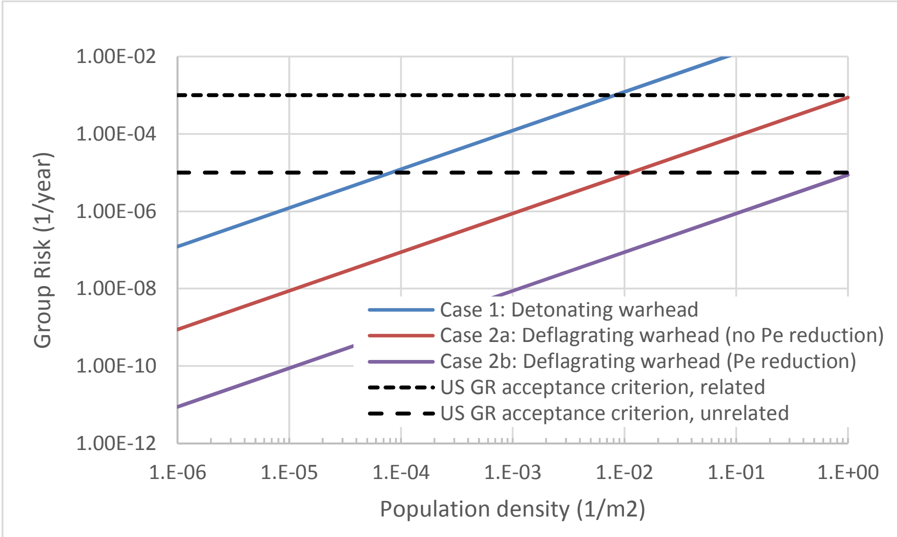

Figure 12: Group Risk (GR) versus population density for case 1, 2a and 2b, compared to US GR acceptance criterion for related and unrelated persons.

The population densities below which the criteria are met are given in Table 4.

Table 4: Case study input and output (continued)

Parameter	Symbol	Case 1	Case 2a	Case 2b
		Detonating warhead	**Deflagrating warhead**	**Deflagrating warhead**
			No Pe reduction	**Pe reduction**
Probability of event (1/year)	Pe	1.00E-5	1.00E-5	1.00E-7
Population density satisfying GR criterion for related persons (1/m^2)	σ_{GR10-3}	1E-2 (1 every 10 by 10 m)	1 (1 every 1 by 1m)	Criterion always met*
Population density satisfying GR criterion for unrelated persons (1/m^2)	σ_{GR10-5}	1E-4 (1 every 100 by 100 m)	1E-2 (1 every 10 by 10 m)	1 (1 every 1 by 1m)

*population density unrealistically large, criterion can be considered always met

This shows that for the detonating warhead the surrounding population density has to be substantially restricted, especially for unrelated persons. For the deflagrating warhead the restrictions are very mild. If the probability reduction (2b) would be applicable the GR would practically not need to be considered at all.

5 CONCLUSIONS

Detonation of a warhead typically leads to well reproducible fragmentation effects. Deflagrations and explosions associated with less violent munitions response still rupture the munition casing, but fragmentation is typically limited to just a few large fragments with a relatively low velocity. Fragmentation modelling has evolved significantly with increasingly realistic predictions, even for less violent explosions and deflagrations.

Although deflagrating warheads produce only a few fragments, these fragments may reach large distances. Reasonable estimates of deflagrating warhead fragment trajectories can be done using plate-like fragments. Conventional safety distances like the MFD and HFD are not well suited for this situation, as MFDs will be very large and HFDs will be relatively small The IR and GR consider a larger amount of relevant aspects such as the ammunition activity and related probability of event, the number of fragments, the population density, and the exposure of both related and unrelated persons. For illustration purposes a simple model was applied to a case study comparing detonating and deflagrating warheads. The case study shows that we can provide reasonable risk estimates for these less violent munition responses. Ultimately, we must answer the question of what is an acceptable risk when throwing a much lower number of lethal fragments to a much longer distance.

REFERENCES

[1] NATO AOP-39, "Policy for Introduction and Assessment of Insensitive Munitions (IM), Edition D Version 1," NATO, Brussels, November 2018.

[2] M. Van der Voort, E. Baker and C. Collet, "Physical Effects and Consequences from Detonations and Less Violent Munition Responses," NATO MSIAC Report L-223, Brussels, Belgium, 2018.

[3] M. Van der Voort, E. Baker and C. Collet, "Physical Effects and Consequences from Detonations and Less Violent Munition Responses," NATO MSIAC Report O-199, Brussels, Belgium, 2018.

[4] C. Collet, E. Baker and M. van der Voort, "History of Natural Fragmentation Models," NATO MSIAC Report L-234, Brussels, Belgium, 2018.

[5] E. Baker, M. Von Ramin and M. van der Voort, "Improved Explosives and Munitions Risk Management Workshop - Focus Area 2B: Fragmentation," NATO MSIAC Report L-234, Brussels, Belgium, 2019.

[6] E. Baker, M. van der Voort and C. Collet, "Fragmentation from Detonations and Less Violent Munition Responses," in *31st International Symposium on Ballistics*, Hyderabad, India, 2019.

[7] M. Van der Voort, "Results of the Improved Explosives and Munitions Risk Management workshop," NATO MSIAC report O-202, Brussels, Belgium, 2019.

[8] V. Gold, "Engineering Model for Design of Explosive Fragmentation Munitions," Technical Report ARAET-TR-07001, US Army ARDEC, Picatinny Arsenal, NJ, USA, 2007.

[9] E. Baker, J. Grau, J. Cordes, E. Vazquez, T. Madsen, D. Suarez, Y. Wu, D. Carlucci and D. Carra, "Analysis of Throw Distance Produced by a Sub-detonative Munition Response," in *Insensitive Munitions & Energetic Material Technology Symposium*, Tucson, AZ, USA, 2009.

[10] T. Kinsey, T. Bussell and C. Chick, "Characterization of Deflagrating Munitions by Rotating Prism High Speed Photography," Technnical Report MRL-TR-91-43, Material Research Laboratory, DSTO, Victoria, Alustralia, 1992.

[11] M. Graswald and W. Arnold, "Experimental Studies of Scalable Effects Warhead Technologies," in *26th International Symposium on Ballistics*, Miami, FL, USA, 2011.

[12] R. Tipton, "CALE Users Manual," Lawerence Livermore National Laboratory, Livermore, CA, USA, 1998.

[13] V. Gold, "Fragmentation Model for Large L/D (Lenght Over Diameter) Explosive Fragmentation Warhead," in *30th Intnernational Symposium on Ballistics*, Long Beach, CA, USA, 2017.

[14] M. Wilkins, "Calculation of Elastic Plastic Flow," *Computational Physics (Academic Press),* vol. 3, 1964.

[15] P. Demmie, "Warhead Fragmentation Modeling with Peridynamics," in *23rd International Symposium on Ballistics*, Tarragona, Spain, 2007.

[16] P. Radles, L. Libersky, T. Carney and F. Sandstrom, "SPH Simulation of Fragmentation in the MK82 Bomb," in *Shock Compression of Condensed Matter - 1995 (AIP Conference Proceedings 370)*, Seattle, WA, USA, 1996.

[17] J. Petit, "An Approach to Generate Random Localizations in Lagrangian Numerical Simulations," in *Materials under Extreme Loadings: Application to Penetration and Impact*, Hoboken, NJ, USA, John Wiley & Sons, Inc., 2010, p. Chapter 14.

[18] M. Ugrcic, "Numerical Simulation of the Fragmentation Process of High Explosive Projectiles," *Scientific Technical Review,* vol. 63, no. 2, pp. 47-57, 2013.

[19] C. Chen, L. Weibing, W. Xiaoming, L. Wenbin and L. Haitao, "Effect of Warhead Shell Thickness on Fragments' Formation and Penetration Performance," in *28th International Symposium on Ballistics*, Atlanta, GA, USA, 2014.

[20] A. Collé, J. Limido, J.-L. Lacome and F. Paintendre, "Innovative Lagrangian Numerical Approach for Natural Fragmentation Modeling," in *29th International Symposium on Ballistics*, Edinburgh, Scotland, UK, 2016.

[21] J. Moxnes, A. Prytz, Ø. Frøyland, S. Børve, S. Skriudalen and G. Ødegårdstuen, "Strain Rate Dependency and Fragmentation Pattern of Expanding Warheads," in *28th International Symposium on Ballistics*, Atlanta, GA, USA, 2014.

[22] M. Graham and S. Bilyk, "Blast Fragmentation Modeling and Analysis," in *27th Army Research Conference*, Orlando, FL, USA, 2010.

[23] J. Chrostowski, W. Gan and L. Cao, "TRAJCAN," ACTA Report No. 14-873/03, Torrance, CA, USA, 2014.

[24] "Technical Paper No. 16, Revision 4, Methodologies for calculating primary fragment Characteristics," Department of Defense Explosives Safety Board, Alexandria, VA, 2012. Restricted.

[25] NATO AASTP-1, "NATO Guidelines for the Storage of Military Ammunition and Explosives," Edition B, Version 1, Brussels, Belgium, December 2015.

[26] NATO AASTP-4, "Explosives Safety Risk Analysis - Part II: Technical Background," Edition 1, Version 4, Brussels, Belgium, 2016.

[27] NATO AASTP-4, "Explosives Safety Risk Analysis - Part I: Guidelines for Risk-Based Decisions," Edition 1, Brussels, Belgium, 2016.